QSAR of adenosine receptor antagonists: Exploring physicochemical requirements for binding of pyrazolo[4,3-*e*]-1,2,4-triazolo[1,5-*c*]pyrimidine derivatives with human adenosine A₃ receptor subtype

D. Pran Kishore [a], C. Balakumar [a], A. Raghuram Rao [a,*], Partha Pratim Roy [b], Kunal Roy [b,*]

[a] Pharmaceutical Chemistry Division, University Institute of Pharmaceutical Sciences and UGC Center of Advanced Study in Pharmaceutical Sciences (UGC-CAS), Panjab University, Chandigarh 160 014, India
[b] Drug Theoretics and Cheminformatics Laboratory, Department of Pharmaceutical Technology, Jadavpur University, Kolkata 700 032, India

ABSTRACT

Human adenosine A₃ receptor (A₃ AR) binding affinity of pyrazolotriazolopyrimidine derivatives ($n = 116$) has been subjected to QSAR analyses using three-dimensional (shape, spatial, electronic, and molecular field) along with thermodynamic descriptors to explore the physicochemical requirements for the binding. QSAR models have been validated internally [using leave-one-out cross-validation method] and externally [using test set molecules] to ensure the predictive capacity of the models. The models suggest that shape of the substituent at N^8 position of the pyrazole ring should be optimum. Furthermore, lipophilic substituents having electronegative atoms at NH₂ group of C^5 position of the pyrimidine ring with distributed negative charge over the surface may enhance the binding affinity. Again, the carbamoylation of the NH₂ group at C^5 position of pyrimidine ring is an essential factor for binding with A₃ receptor. The QSAR models were used for the design and development of some novel thienopyrimidines which were predicted to have good affinity towards A₃ AR.

© 2010 Elsevier Ltd. All rights reserved.

Adenosine receptors (ARs), classified as A₁, A₂A, A₂B, and A₃ subtypes[1] and belonging to the super family of G-protein coupled receptors (GPCRs) have emerged as potential drug targets. They play a significant role in a number of varied biological functions.[2] The discovery of selective ligands (agonists[3] and antagonists[4]) has facilitated understanding of the tissue distribution and the role of each receptor subtype. In particular, the A₃ AR has been recently cloned from different species such as rat, human, sheep, mouse, dog, and rabbit.[5–10] Significant differences in sequence homology (72%) for A₃ receptors have been observed between species.[8] The amino acid sequence of the human A₃ AR is 49.5%, 43.2%, and 39.9% identical in sequence to human A₁, A₂A, and A₂B AR, respectively. Among the various species, rat A₃ AR is significantly different from human (73.8% of identical sequence), whereas sheep A₃ AR is closely related to the human receptor (85.2% of identical sequence).[11] The rat A₃ AR in particular behaves anomalously in ligand binding assays with different affinities for same ligands (antagonists) versus human A₃ AR.[12] Furthermore, tissue distribution of A₃ AR is very different in rat as compared to man. In rat, A₃ AR is expressed in high density in testis and mast cells and lower density in most other tissues. In human, highest A₃ receptor densities are found in lungs, liver, and cells of the immune system (neutrophils, eosinophils, T-lymphocytes), but not on mast cells. Lower levels have been detected in many other human tissues, including brain, heart, and testis.[13]

A₃ AR activation has been shown to positively modulate phospholipases C[14,15] and D,[15,16] K_ATP channel,[16] inositol triphosphate (IP₃),[17] and intracellular calcium[17,18], and inhibit adenylate cyclase.[1] Activation of this receptor subtype also leads to modulation of mitogen-activated protein kinases (MAPK), such as the extracellular signal-regulated kinase (ERK) 1/2 and the stress-activated protein kinase p38.[19] The A₃ regulation of the cell cycle may induce cell protection or cell death, depending on the degree of receptor activation and/or the cell type or the toxic insult.[19–21] As a consequence of this dual effect, both A₃ receptor agonists and antagonists might be effective therapeutics in cancer.[22–24]

The growing understanding of the physiological effects mediated by the A₃ subtype, such as modulation of cerebral and cardiac ischemia,[11,25] inflammation,[26] or normal and tumor cell regulation,[22–24] makes this receptor subtype an interesting target for various therapeutic interventions.[2,13] In particular, highly selective A₃ AR antagonists are being investigated as potential antiasthmatic,[26] anti-inflammatory,[26] antiglaucoma,[27] and cerebroprotective agents,[28,29] and recently, they have been described as potential therapeutics in the treatment of glioblastoma multiforme,[24] colon

* Corresponding authors. Tel.: +91 172 2534111; fax: +91 172 2543101 (A.R.R.); tel.: +91 9831594140; fax: +91 33 2837 1078 (K.R.).
E-mail addresses: rrakkinepally@pu.ac.in (A. Raghuram Rao), kunalroy_in@yahoo.com (K. Roy).

cancer,[30] and renal injury.[31] However, concerning specifically the potential treatment of inflammation and asthma, the role of both A_3 agonists and antagonists is still ambiguous.[21,32]

In recent years, much effort has been directed toward searching for potent and selective human A_3 adenosine antagonists.[2–4,2b] Some recent developments in this field comprise the identification of 1,2,4-triazolo[1,5-*i*]purines,[33] 1,2,4-triazolo[4,3-*a*]quinoxalin-1-ones,[34,35] thiazoles and thiadiazoles,[36,37] imidazo[2,1-*i*]purin-5-ones,[4b] pyrido[2,1-*f*]purine-2,4-dione,[38] pyrazolo[3,4-*c*]/[4,3-*c*] quin olin-4-ones,[39,40] triazolothienopyrimidines,[41] pyrazolo-triaz-olo-pyrimidines,[42] adenosine derivatives,[43–45] and xanthine derivatives.[46] But only a few such compounds are currently undergoing clinical trials for the treatment of several diseases because of unde-sirable side effects of other compounds due to the wide distribution of ARs, low water solubility of the compounds, or lack of effects in some cases perhaps due to low receptor density in the targeted tissue.[47]

In addition, the design, development, and commercialization of a drug is a tedious, time consuming and cost-intensive process. For these reasons, any tool or technique that increases the efficiency of any stage of the drug discovery process is highly desirable. As the main paradigm of medicinal chemistry is that the biological activ-ity, as well as physical, physicochemical, and chemical properties, of organic compounds depends on their molecular structure, com-puter-aided drug design based on Quantitative Structure Activity Relationship (QSAR) methods is one such tool that can be used to increase the efficiency of the drug discovery process.[48,49]

In the past decades, QSAR studies have been done on various derivatives such as flavoniods,[50] pyrazolotriazolopyrimidines,[42] quinoxalines,[51,52] quinolines,[53] 1,2,4-triazolo[5,1-i]-purine deriva-tives,[54] pyridine derivatives,[55] thiazole and thiadiazole ana-logues,[56,57] to study their affinity for A_3 AR.

Recently, Moro et al.[42] published an interesting prediction strat-egy for the design of new antagonists by combining target-based and ligand-based drug design approaches to define a novel phar-macophore model for the human A_3 receptor. High throughput molecular docking and Comparative Molecular Field Analysis (CoMFA) were used in tandem to assemble a new target-based pharmacophore model. A total of 106 pyrazolotriazolopyrimidine derivatives were included in the training set to generate the QSAR model for human A_3 receptors. On the basis of this strategy, they have designed, synthesized, and tested 17 new derivatives and subsequently used them as the test set to evaluate the predictive power of the CoMFA model.

In the present communication, further QSAR studies have been performed using the binding affinities (inhibitory activities) of 116 pyrazolo[4,3-*e*]-1,2,4-triazolo[1,5-*c*]pyrimidine derivatives[42] (Fig. 1) as a model data set (eliminating seven compounds **38–40**, **101**, **103**, **105**, and **106** as outliers based on preliminary QSAR model development and residual analyses) with 3D (shape, spatial, electronic, and molecular field) along with thermodynamic descriptors to get a deep insight into the SARs required for selec-tive binding towards A_3 AR. The biological activity data of these

116 compounds [Ki(nM)] were converted to logarithmic scale [pKi(mM)] and then used for subsequent QSAR analyses as the re-sponse variable. There are only two regions of structural variations in the compounds, which are R^1 at C^5 position of pyrimidine moi-ety and R at N^8 position of pyrazole moiety. The structural features and biological activity values of the compounds are presented in Table S1 in Supplementary Materials section.

The categorical list of descriptors used in the development of QSAR models is reported in Table S2 in Supplementary Materials section. For the calculation of 3D descriptors, multiple conforma-tions of each molecule were generated using the optimal search as a conformational search method. Each conformer was subjected to an energy minimization procedure using smart minimizer under open force field (OFF) to generate the lowest energy conformation for each structure. The charges were calculated according to the Gasteiger method. All the descriptors were calculated using Descriptor+ module of the Cerius2 version 4.10 software running on a Silicon Graphics workstation.[58]

The robustness of the QSAR models are generally verified by using different types of validation criteria such as (i) internal vali-dation or cross-validation, (ii) validation by dividing the dataset into training and test compounds, (iii) data randomization or Y-scrambling, and (iv) true external validation by application of model on new external data.[59] In the present work, due to the lack of true external evaluation set, the total dataset ($n = 116$) has been divided into training ($n = 86$) and test (external evaluation) ($n = 30$) (75% and 25%, respectively, of the total number of compounds) sets based on clusters obtained from *k*-means clustering[60,61] applied on standardized physicochemical, structural, and spatial descriptor matrix. All the parameters (physicochemical and spatial descrip-tors) were standardized and the whole dataset was clustered into four subgroups from each of which 25% of compounds were selected as members of the test set. Serial numbers of compounds under different clusters are presented in Table S3 in Supplementary Materials section.

The 3D-QSAR models developed from the training set were internally cross-validated using leave-one-out (LOO) method with LOO-Q^2 metric.[62] However, internal validation does not ascertain that the model will perform well on a new set of data. Thus, the whole data set was divided into training and test sets and the mod-els developed from the training set were externally validated based on external predictions for the test set molecules using the predic-tive R^2 (R^2_{pred}) metric.[63] The models were also validated using data randomization or Y-scrambling technique.[59] An additional param-eter r^2_m (defined as $r^2 * (1 - \sqrt{r^2 - r^2_0})$, r^2 and r^2_0 being squared cor-relation coefficients between observed and predicted values of the compounds), which penalizes a model for large differences be-tween observed and predicted values, was also calculated.[64] Two variants of r^2_m parameter, $r^2_{m(LOO)}$ and $r^2_{m(test)}$, which penalize a model more strictly than Q^2 and R^2_{pred}, respectively, were calculated.[65] In case of good prediction, where the predicted activity values lie in close proximity to the observed data, the r^2 value will be very near to the r^2_0 value. Consequently, an ideal prediction of activity is char-acterized by a value of r^2_m equal to that of r^2. The $r^2_{m(LOO)}$ and $r^2_{m(test)}$ metrics are used for detecting proximity of the predicted activity data to that of the observed ones for the training and test sets, respectively. Besides these, the $r^2_{m(overall)}$ metric[65] was also calcu-lated which ascertains the overall model predictivity based on the predicted property values of the whole dataset (both training and test sets). The $r^2_{m(overall)}$ metric helps to identify the best model from among comparable models, especially when different models show different patterns in internal and external predictivity. Another metric ${}^cR^2_p$ (${}^cR^2_p = R * \sqrt{R^2 - R^2_r}$) ($R^2_r$ being squared mean
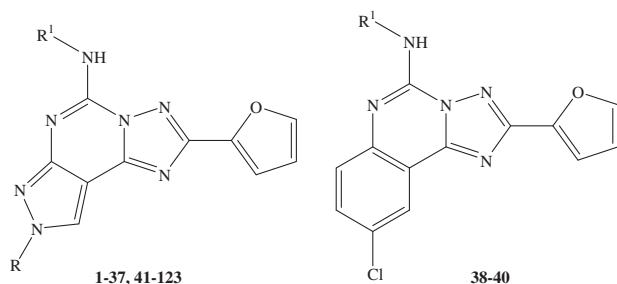

Figure 1. General structures of the pyrazolotriazolopyrimidines.

1-37, 41-123

38-40

correlation coefficient of random models) was also calculated[66] to check whether the models thus developed are not obtained by chance.

3D-QSAR studies have been performed to obtain information about the effect of shape, spatial arrangement of atoms in three-dimensional space and charge distribution of the substituents on the A_3 binding affinity. This study was conducted using molecular shape analysis (MSA) descriptors along with additional descriptors like physicochemical, spatial, and electronic parameters. Figure 2 shows the aligned geometry of the training set compounds used in MSA. Initially MSA has been performed[2b,65,67] by generating the conformers using the 'optimal search' method available in Cerius2 version 4.10 software.[58] Models have been generated with shape, spatial, and electronic descriptors using GFA with linear option as the statistical tool.[68] The mutation probability was kept at 5000 iterations. Smoothness (d) was kept at 1.00. Initial equation length value was selected as 4 and the length of the final equation was not fixed. In case of GFA linear technique the following equation was obtained with acceptable LOO internal variance (Q^2) and external predicted variance (R^2_{pred}).

Jurs_RNCG is the partial charge of the most negative atom divided by the total negative charge.

$$RNCG = \frac{Q^-_{max}}{Q^-}$$

Q^-_{max} =charge of the most negative atom, Q^- =total negative charge.

Jurs_RNCG has unfavorable contribution towards the affinity as evidenced by the negative regression coefficient. This indicates that if the negative charge concentrates at a particular atom then the activity may be diminished. This can be evident from certain derivatives of the dataset such as compound number **3**, **6**, **9**, **12**, **16**, **19**, **22**, **25**, **28**, **31**, **34**, **37**, **42** etc. where their binding affinities were smaller compared to the other derivatives of the series due to the presence of highly electronegative chlorine atom at R^1 position. So, for better activity, negative charge should be optimum and distributed over the surface as observed from the compounds such as **2**, **5**, **8**, **11**, **15**, **18** etc.

Jurs-DPSA-2 is the total charge weighted positive solvent-accessible surface area minus the total charge weighted negative solvent-accessible surface area, that is,

$$pK_i = 28.530(\pm2.583) + 1.230(\pm0.161)\text{shapeRMS} - 0.004(\pm0.001)\text{jurs-DPSA} - 2$$
$$- 0.016(\pm0.002)\text{NCOSV} - 104.459(\pm10.97)\text{jurs-RNCG} + 0.005(\pm0.002)\text{jurs-TASA} + 0.264(\pm0.116)A\log P$$
$$n_{training} = 86, LOF = 0.377, R^2 = 0.779, R^2_a = 0.762, F = 43.25(df6, 79), s = 0.551,$$
$$\text{PRESS} = 29.468, Q^2 = 0.728, r^2_{m(LOO)} = 0.546, n_{Test} = 30, R^2_{pred} = 0.760,$$
$$r^2_{m(test)} = 0.747 r^2_{m(overall)} = 0.589 \tag{M1}$$

The standard errors (SE) of the regression coefficients are shown within parentheses. The above model could explain 76.2% of the variance (adjusted coefficient of variation-R^2_a). The leave-one-out predicted variance (Q^2) was found to be 72.84%. The predictive potential of this model was determined by predicted R^2 of the test set compounds and it was found to be 76% (Fig. S1 in Supplementary Materials section). The r^2_m values for the test, training and overall sets were found to be 0.747, 0.546, and 0.589, respectively, as listed in Table 1.

Shape RMS is the root mean square deviation between the individual molecule and the shape reference compound. It has a positive contribution toward the binding affinity and increase in the value of Shape RMS may increase the affinity as is the case for compounds **5**, **8**, **11**, **15** etc.
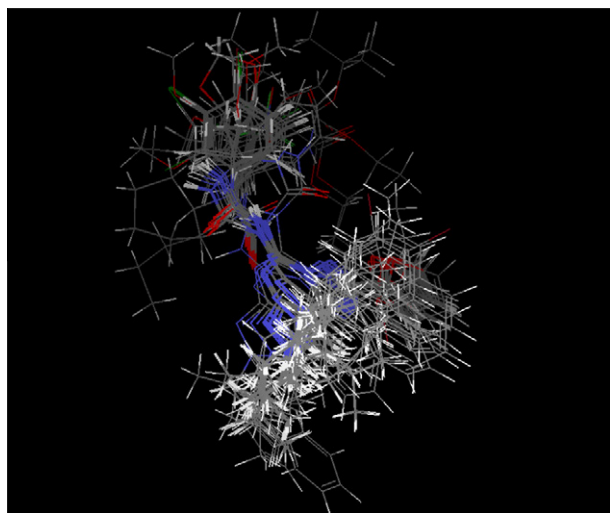
$$DPSA_2 = PPSA_2 - PNSA_2$$

Jurs-DPSA-2 has unfavorable contribution to the binding affinity as evidenced by the negative regression coefficient. This has been already supported by the descriptor Jurs_RNCG as described above.

NCOSV is the volume of the individual molecule and the common overlap steric volume. It has a detrimental contribution towards the activity as evidenced by the negative regression coefficient. If the non-common volume of any molecule differs from the shape reference compound to a large extent, the binding affinity may reduce.

Jurs-TASA is the sum of solvent-accessible surface areas of atoms with absolute value of partial charges less than 0.2, that is,

$$TASA = \sum_a SA_a$$
$$\forall_a : |q_a| < 0.2$$

Jurs-TASA has a favorable contribution toward the affinity as evidenced by the positive regression coefficient.

$A\log P$ is calculated using the method described by Ghose and Crippen.[69] It has a positive contribution towards A_3 ARs binding affinity. This reveals that increase in the lipophilicity of ligands may enhance the binding affinity. This has been already supported by the previous descriptor, that is, Jurs-TASA.

Molecular field analysis (MFA) is a method for quantifying the interaction energy between a probe molecule and a set of aligned target molecules in QSAR.[70] Figure 3 shows the aligned geometry of the most active compound (compound **2**) within the MFA grid showing the important interaction points. MINITAB[73] was used for linear regression and PLS techniques. In case of G/PLS spline technique[58,71,72] the following equation was obtained with satisfactory LOO internal variance (Q^2) and predicted variance (R^2_{pred}) values (Fig. S2 in Supplementary materials section). Statistical quality of the M2 along with other models listed in Table 1.

The parameter $CH_3/677$ indicates the interaction of the steric probe CH_3 at grid point number 677 with the molecules. It has a

Figure 2. Aligned geometry of the training set compounds used in MSA.

Table 1
Comparative table of statistical qualities of different models.

Statistical technique	Model	R^2	Q^2	R^2_{pred}	$r^2_{m(test)}$	$r^2_{m(LOO)}$	$r^2_{m(overall)}$
GFA	M1	0.779	0.728	0.760	0.747	0.546	0.589
G/PLS	M2	0.797	0.762	0.662	0.630	0.583	0.593
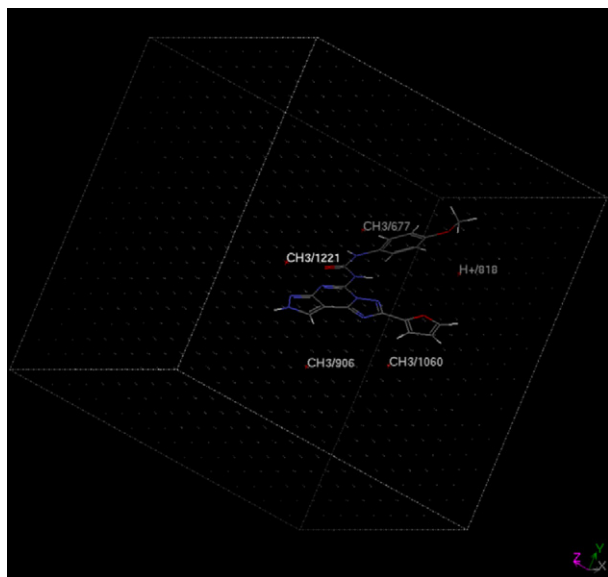
Figure 3. Aligned geometry of the most active compound **2** within the MFA grid showing the important interaction points.

small substituent or absence of any substitution at N^8 and C^9 may be favorable for retaining the binding affinity as already supported by the earlier descriptor $CH_3/1221$.

The term $CH_3/1060$ indicates the interaction of the steric probe at grid point number 1060 with the molecules. It is present as a spline term and has a positive effect to the binding affinity. The value of $CH_3/1060$ should be less than 0.323 to nullify this effect. Interaction with CH_3 at the grid point 1060 is possible only with the furan ring attached at C2 position of the triazole ring. This indicates that the presence of furan ring may be an essential factor in retaining the binding affinity.

The term $H^+/818$ indicates the interaction of the electropositive probe at grid point number 1060 with the molecules. It is present as a spline variable and has a positive effect to the binding affinity. The value of $H^+/818$ should be greater than 1.884 to increase the binding affinity. It indicates that the presence of electronegative substituents at positions 3 and 4 of the phenyl ring of aromatic carbamoyl group attached to C^5 of the pyrimidine ring, may increase the binding affinity as observed from the compounds **3**, **5**, **6**, **44**, **48** etc. Again, absence of electronegative substitution at the above mentioned positions may reduce the binding affinity as indicated from the compounds **107** and **108**.

Alkyl substitution with carbon chain length up to C^4 at N^8 position of pyrazole ring and carbamoylation of amino group (at C^5 po-

$$pK_i = 3.914 - 0.045CH_3/677 - 0.025CH_3/1221 - 0.020CH_3/906 + 1.872 < 0.323 - CH_3/1060 > +0.006 < H^+/818 + 1.884 >$$
$$n_{training} = 86, LSE = 0.197, R^2 = 0.797, R^2_a = 0.789, F = 107.42(df\,3,82), s = 0.518,$$
$$PRESS = 25.866, Q^2 = 0.726, r^2_{m(LOO)} = 0.583, n_{Test} = 30, R^2_{pred} = 0.662, r^2_{m(test)} = 0.630, r^2_{m(overall)} = 0.583 \tag{M2}$$

positive effect on the binding affinity. Significant interaction at this grid point occurs only in case of high steric volume of substituents at the R^1 substitution position. This implies that unsubstituted amino group at C^5 of the pyrimidine ring may reduce the binding affinity as evident from compounds such as **1**, **4**, **7**, **10**, **14**, **17**, **20**, **23**, **26**, **29**, **32**, **35** etc. On the other hand, the carbamoylation of 5-amino group (R^1) to yield urea derivatives (e.g. **2**, **3**, **5**, **6**, **8**, **9**, **11**, **12**, **13** etc.), may increase the affinity and selectivity towards A_3 AR at subnanomolar range.

The term $CH_3/1221$ represents the interaction of the steric probe at grid point number 1221 with the molecules. It has a unfavorable contribution to the binding affinity. Interaction with CH_3 at the grid point 1221 is possible when a long chain substituent is present at the R position of N^8. This can be encountered in case of compounds **20** to **37**. These compounds have long chain substituent at the R position, so their activity is less. It has been observed that increase in carbon chain length beyond C4 at substitution position R reduces the binding affinity.
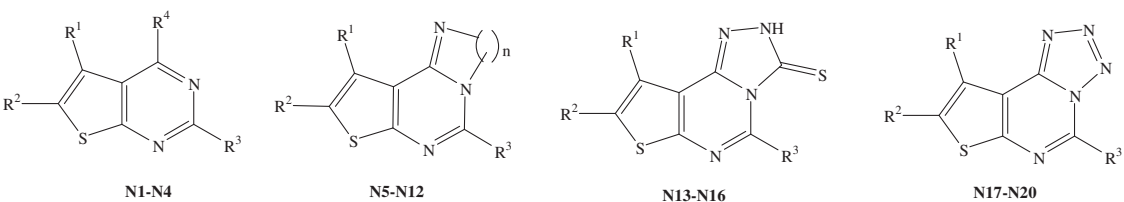
The term $CH_3/906$ indicates the interaction of the steric probe at grid point number 906 with the molecules. It has a negative effect on the binding affinity. Interaction with CH_3 at the grid point 906 is possible when a long chain substituent is present at the N^8 or C^9 position of pyrazole ring. It indicates that the presence of either

sition of pyrimidine ring) with aromatic amide having substituents with electronegative atoms at 3rd and 4th position of the phenyl ring may increase the binding affinity towards A_3 ARs.

The results of the randomization tests for the process of model development and models are listed in Table S4 in Supplementary Materials section. Based on model randomization, the $^cR^2_p$ values for the process and developed models are well above the cut off value (>0.5) indicating the models are not obtaining by chance.

From the dataset (Table S1 in Supplementary Materials section), it is evident that the most active compounds **2** and **39** with same activity (hA_3K_i: 0.14 nM) have the same scaffold except the former contains a pyrazole moiety and the later contains a p-chlorobenzene moiety. So, the role of pyrazole and benzene moieties in inducing the binding affinity towards A_3 AR is not clear. Further, the literature shows that antagonists of A_1 AR possess quite good affinities for the A_3 AR and scarce A_1 versus A_3 selectivity.[74] The benzene ring of a biologically active compound may often be replaced by a thiophene without loss of activity.[75] Thus, to develop a new class of compounds targeting the A_3 AR, but with a better affinity and selectivity profile, it is thought of interest to go for bioisosteric replacement of pyrazole moiety of compound **2** and benzene ring of compound **39** with thiophene moiety. Recently, a series of triazolothienopyrimidines has been reported[41] from our

Table 2
Probable A_3 ARs binding affinities of designed hetero-fused thienopyrimidines based on MSA (M1) and MFA (M2) models

Compd No.	R^1	R^2	R^3	R^4	n	Predicted activity (pK_i = nM)	
						MSA	MFA
N1	CH_3	CH_3	$-NHCOC_6H_5$	$-OH$	—	2.87	5.24
N2	$-(CH_2)_3-$		$-NHCOC_6H_5$	$-OH$	—	2.90	4.70
N3	$-(CH_2)_4-$		$-NHCOCH_3$	$-OH$	—	0.83	6.76
N4	$-(CH_2)_4-$		$-NHCOC_6H_5$	$-OH$	—	3.17	4.03
N5	CH_3	CH_3	$-NHCOC_6H_5$	—	2	5.38	6.33
N6	CH_3	CH_3	$-NHCOC_6H_5$	—	3	5.04	6.34
N7	$-(CH_2)_3-$		$-NHCOC_6H_5$	—	2	5.44	6.33
N8	$-(CH_2)_3-$		$-NHCOC_6H_5$	—	3	5.08	6.35
N9	$-(CH_2)_4-$		$-NHCOC_6H_5$	—	2	5.63	6.35
N10	$-(CH_2)_4-$		$-NHCOC_6H_5$	—	3	5.27	6.37
N11	$-(CH_2)_4-$		$-NHCOCH_3$	—	2	4.46	6.26
N12	$-(CH_2)_4-$		$-NHCOCH_3$	—	3	4.22	4.30
N13	CH_3	CH_3	$-NHCOC_6H_5$	—	—	7.40	7.13
N14	$-(CH_2)_3-$		$-NHCOC_6H_5$	—	—	7.41	3.98
N15	$-(CH_2)_4-$		$-NHCOC_6H_5$	—	—	7.45	7.23
N16	$-(CH_2)_4-$		$-NHCOCH_3$	—	—	5.31	4.26
N17	CH_3	CH_3	$-NHCOC_6H_5$	—	—	4.08	7.88
N18	$-(CH_2)_3-$		$-NHCOC_6H_5$	—	—	4.16	7.88
N19	$-(CH_2)_4-$		$-NHCOC_6H_5$	—	—	7.45	7.23
N20	$-(CH_2)_4-$		$-NHCOCH_3$	—	—	5.31	4.26

laboratories as adenosine A_1 receptor antagonists at micromolar (μM) ranges and none of them showed affinity towards A_{2A} AR. The encouraging results prompted us to further design a series of some novel hetero-fused thienopyrimidines (Table 2) as bioisosters of pyrazolotriazolopyrimidines and triazoloquinazolines as possible A_3 AR antagonists with better affinity and selectivity profile.

Based on the best models developed by MSA [model M1] and MFA [model M2], probable A_3 AR binding affinities of some hetero-fused thienopyrimidines (Table 2) such as pyrimidothienopyrimidines, imidazothienopyrimidines, triazolothienopyrimidines, and tetrazolothienopyrimidines have been predicted. Triazolothienopyrimidines with carbamoyl substitution at NH_2 group at C^5 position of pyrimidine ring were predicted to have very high affinity towards A_3 ARs compared to other mentioned hetero-fused thienopyrimidines. Synthesis and biological evaluation of these designed compounds are in progress.

In conclusion, QSAR studies have been carried out for the binding affinity of pyrazolotriazolopyrimidines towards A_3 AR using both 2D (physicochemical and structural) and 3D (shape, spatial, electronic, and molecular field) descriptors. The chemometric tools used for the analyses are Genetic Function Approximation (GFA) and Genetic Partial Least Squares (G/PLS). The whole dataset (n = 116) was divided into a training set (75% of the dataset) and a test set (remaining 25%) on the basis of k-means clustering of standardized physicochemical, structural and spatial descriptor matrix. Models developed from the training set were used to predict the binding affinity of the test set compounds. All the models have been validated internally and externally. Among the 3D parameters, spatial (Jurs_RNCG, Jurs_TASA_3, and Jurs_DPSA-2), and shape (NCOSV, ShapeRMS) descriptors showed importance. Along with the 3D descriptors, hydrophobicity ($A \log P$) emerged as an important descriptor. MFA suggests the importance of probes (H^+, CH_3) at definite locations. The MSA model [model M1] was

found to be the best model on the basis of highest external ($R^2_{\text{pred}} = 0.760$) predictive potential and $r^2_{\text{m(overall)}}$ criteria. Similarly, the MFA model [model M2] was found to be the best model among all the derived models, on the basis of highest internal ($Q^2 = 0.762$) predictive potential. The developed models suggest that shape of the substituent should be optimum at N^8 position of pyrazole ring and lipophilic substituents having electronegative atoms at NH_2 group of C^5 position of pyrimidine ring with distributed negative charge over the surface may enhance the affinity towards A_3 AR. It has been observed that the carbamoylation of NH_2 group at C^5 position of pyrimidine ring is an essential factor for higher affinity with selectivity towards A_3 receptor. The best models developed by MSA [model M1] and MFA [model M2] were used for the design and development of novel compounds (thienopyrimidines) which have been predicted to have better affinity towards A_3 AR. Efforts are in progress to synthesise the designed compounds following appropriate synthetic schemes as well as to evaluate them for their affinity and selectivity as A_3 AR antagonists and the results will be reported in future.

Acknowledgments

Supplementary data

Supplementary data associated with this article can be found, in the online version, at doi:10.1016/j.bmcl.2010.11.094.

References and notes

1. Fredholm, B. B.; Ijzerman, A. P.; Jacobson, K. A.; Klotz, K. N.; Linden, J. *Pharmacol. Rev.* **2001**, *53*, 527.
2. (a) Jacobson, K. A.; Gao, Z. G. *Nat. Rev. Drug Disc.* **2006**, *5*, 247; (b) Moro, S.; Gao, Z. G.; Jacobson, K. A.; Spalluto, G. *Med. Res. Rev.* **2006**, *26*, 131; (c) Muller, C. E.; Scior, T. *Pharm. Acta Helv.* **1993**, *68*, 77.
3. (a) Muller, C. E. *Curr. Med. Chem.* **2000**, *7*, 1269; (b) Keeling, S. E.; Albinson, F. D.; Ayres, B. E.; Butchers, P. R.; Chambers, C. L.; Cherry, P. C.; Ellis, F.; Ewan, G. B.; Gregson, M.; Knight, J.; Mills, K.; Ravenscroft, P.; Reynolds, L. H.; Sanjar, S.; Sheehan, M. J. *Bioorg. Med. Chem. Lett.* **2000**, *10*, 403.
4. (a) Muller, C. E. *Drugs Future* **2000**, *25*, 1043; (b) Muller, C. E.; Thorand, M.; Qurishi, R.; Diekmann, M.; Jacobson, K. A.; Padgett, W. L.; Daly, J. W. *J. Med. Chem.* **2002**, *45*, 3440; (c) Muller, C. E. *Mini-Rev. Med. Chem.* **2001**, *1*, 433.
5. Meyerhof, W.; Brechlin, R. M.; Richter, D. *FEBS Lett.* **1991**, *284*, 155.
6. Sajjadi, F. G.; Firestein, G. S. *Biochim. Biophys. Acta* **1993**, *1179*, 105.
7. Salvatore, C. A.; Jacobson, M. A.; Taylor, H. E.; Linden, J.; Johnson, R. G. *Proc. Natl. Acad. Sci. U.S.A.* **1993**, *90*, 10365.
8. Linden, J.; Taylor, H. E.; Robeva, A. S.; Tucker, A. L.; Stehle, J.; Rivkees, S. A.; Fink, J. S.; Reppert, S. M. *Mol. Pharmacol.* **1993**, *44*, 524.
9. Zhao, Z. H.; Ravid, K. *Genomics* **1995**, *30*, 118.
10. Hill, R. J.; Oleynek, J. J.; Hoth, C. F.; Kiron, M. A.; Weng, W. F.; Wester, R. T.; Tracey, W. R.; Knight, D. R.; Buchholz, R.; Kennedy, S. P. *J. Pharmacol. Exp. Ther.* **1997**, *280*, 122.
11. Linden, J. *Trends Pharmacol. Sci.* **1994**, *15*, 298.
12. (a) Jacobson, K. A. *Trends Pharmacol. Sci.* **1998**, *19*, 184; (b) Baraldi, P. G.; Cacciari, B.; Moro, S.; Romagnoli, R.; Xiao-duo, J.; Jacobson, K. A.; Gessi, S.; Borea, P. A.; Spalluto, G. *J. Med. Chem.* **2001**, *44*, 2735.
13. Muller, C. E. *Curr. Top. Med. Chem.* **2003**, *3*, 445.
14. Abbracchio, M. P.; Brambilla, R.; Kim, H. O.; Jacobson, K. A.; Cattabeni, F. *Mol. Pharmacol.* **1995**, *48*, 1083.
15. Parsons, M.; Young, L.; Lee, J. E.; Jacobson, K. A.; Liang, B. T. *FASEB J.* **2000**, *14*, 1423.
16. Ali, H.; Choi, O. H.; Fraundorfer, P. F.; Yamada, K.; Gonzaga, H. M. S.; Beaven, M. A. *J. Pharmacol. Exp. Ther.* **1996**, *276*, 837.
17. Shneyvays, V.; Leshem, D.; Zinman, T.; Mamedova, L. K.; Jacobson, K. A.; Shainberg, A. *Am. J. Physiol. Heart Circ. Physiol.* **2005**, *288*, 2792.
18. Englert, M.; Quitterer, U.; Klotz, K. N. *Biochem. Pharmacol.* **2002**, *64*, 61.
19. Schulte, G.; Fredholm, B. B. *Cell. Signalling* **2003**, *15*, 813.
20. Brambilla, R.; Cattabeni, F.; Ceruti, S.; Barbieri, D.; Franceschi, C.; Kim, Y.-C.; Jacobson, K. A.; Klotz, K. N.; Lohse, M. J.; Abbracchio, M. P. *Arch. Pharmacol.* **2000**, *361*, 225.
21. Gessi, S.; Merighi, S.; Varani, K.; Leung, E.; Mac Lennan, S.; Borea, P. A. *Pharmacol. Ther.* **2008**, *117*, 123.
22. Merighi, S.; Mirandola, P.; Varani, K.; Gessi, S.; Leung, E.; Baraldi, P. G.; Tabrizi, M.; Borea, P. A. *Pharmacol. Ther.* **2003**, *100*, 31.
23. Madi, L.; Ochaion, A.; Wolfson, R. L.; Yehuda, S. B.; Erlanger, A.; Ohana, G.; Harish, A.; Merimski, O.; Barer, F.; Fishman, P. *Clin. Cancer Res.* **2004**, *10*, 4472.
24. Merighi, S.; Benini, A.; Mirandola, P.; Gessi, S.; Varani, K.; Leung, E.; Maclennan, S.; Borea, P. A. *Biochem. Pharmacol.* **2006**, *72*, 19.
25. Liang, B. T.; Jacobson, K. A. *Proc. Natl. Acad. Sci. U.S.A.* **1998**, *95*, 6995.
26. Young, H. W.; Molina, J. G.; Dimina, D.; Zhong, H.; Jacobson, M.; Chan, L. N.; Chan, T. S.; Lee, J. J.; Blackburn, M. R. *J. Immunol.* **2004**, *173*, 1380.
27. Okamura, T.; Kurogi, Y.; Hashimoto, K.; Sato, S.; Nishikawa, H.; Kiryu, K.; Nagao, Y. *Bioorg. Med. Chem. Lett.* **2004**, *14*, 3775.
28. Brambilla, R.; Cattabeni, F.; Ceruti, S.; Barbieri, D.; Franceschi, C.; Kim, Y.-C.; Jacobson, K. A.; Klotz, K.-N.; Lohse, M. J.; Abbracchio, M. P. *Arch. Pharmacol.* **2000**, *361*, 225.
29. Pugliese, A. M.; Coppi, E.; Spalluto, G.; Corradetti, R.; Pedata, F. *Br. J. Pharmacol.* **2006**, *147*, 524.
30. Gessi, S.; Cattabriga, E.; Avitabile, A.; Gafa, R.; Lanza, G.; Cavazzini, L.; Bianchi, N.; Gambari, R.; Feo, C.; Liboni, A.; Gullini, S.; Leung, E.; Lennan, S. M.; Borea, P. A. *Clin. Cancer Res.* **2004**, *10*, 5895.
31. Lee, H. T.; Setlik, A. O.; Xu, H.; Agati, V. D.; Jacobson, M. A.; Emala, C. W. *Am. J. Physiol. Renal Physiol.* **2003**, *284*, 267.
32. Wilson, C. N. *Br. J. Pharmacol.* **2008**, *155*, 475.
33. Okamura, T.; Kurogi, Y.; Nishikawa, H.; Hashimoto, K.; Fujiwara, H.; Nagao, Y. *J. Med. Chem.* **2002**, *45*, 3703.
34. Colotta, V.; Catarzi, D.; Varano, F.; Cecchi, L.; Filacchioni, G.; Martini, C.; Trincavelli, L.; Lucacchini *J. Med. Chem.* **2000**, *43*, 1158.
35. Colotta, V.; Catarzi, D.; Varano, F.; Calabri, F. R.; Lenzi, O.; Filacchioni, G.; Martini, C.; Trincavelli, L.; Deflorian, F.; Moro, S. *J. Med. Chem.* **2004**, *47*, 3580.
36. Jung, K. Y.; Kim, S. K.; Gao, S. K.; Gross, Z. G.; Melman, A. S.; Jacobson, K. A.; Kim, Y. C. *Bioorg. Med. Chem.* **2004**, *12*, 613.
37. Press, N. J.; Keller, T. H.; Tranter, P.; Beer, D.; Jones, K.; Faessler, A.; Heng, R.; Lewis, C.; Howe, T.; Gedeck, P.; Mazzoni, L.; Fozard, J. R. *Curr. Top. Med. Chem.* **2004**, *4*, 863.
38. Priego, E. M.; Kuenzel, V. D.; Ijzerman, A. P.; Camarasa, M. J.; Perez, M. P. *J. Med. Chem.* **2002**, *45*, 3337.
39. Colotta, V.; Catarzi, D.; Varano, F.; Capelli, F.; Lenzi, O.; Filacchioni, G.; Martini, C.; Trincavelli, L.; Ciampi, O.; Pugliese, A. M.; Pedata, F.; Schiesaro, A.; Morizzo, E.; Moro, S. *J. Med. Chem.* **2007**, *50*, 4061.
40. Baraldi, P. G.; Tabrizi, M. A.; Preti, D.; Bovero, A.; Fruttarolo, F.; Romagnoli, R.; Zaid, N. A.; Moorman, A. R.; Varani, K.; Borea, P. A. *J. Med. Chem.* **2005**, *48*, 5001.
41. Raghu Prasad, M.; Rao, A. R.; Rao, P. S.; Rajan, K. S.; Meena, S.; Madhavi, K. *Eur. J. Med. Chem.* **2008**, *43*, 614.
42. Moro, S.; Paolo, B.; Francesca, D.; Cristina, F.; Pastorin, G.; Cacciari, B.; Baraldi, P. G.; Varani, K.; Borea, P. A.; Spalluto, G. *J. Med. Chem.* **2005**, *48*, 152.
43. Gao, Z. G.; Joshi, B. V.; Klutz, A. M.; Kim, S. K.; Lee, H. W.; Kim, H. O.; Jeong, L. S.; Jacobson, K. A. *Bioorg. Med. Chem. Lett.* **2006**, *16*, 596.
44. Jeong, L. S.; Choe, S.; Gunaga, P.; Kim, H. O.; Lee, H. W.; Lee, S. K.; Tosh, D. K.; Patel, A.; Palaniappan, K. K.; Gao, Z. G.; Jacobson, K. A.; Moon, H. R. *J. Med. Chem.* **2007**, *50*, 3159.
45. Jeong, L. S.; Lee, H. W.; Kim, H. O.; Tosh, D. K.; Pal, S.; Choi, W. J.; Gao, Z. G.; Patel, A. R.; Williams, W.; Jacobson, K. A.; Kim, H. D. *Bioorg. Med. Chem. Lett.* **2008**, *18*, 1612.
46. Drabczyn, A.; Schumacher, B.; Müller, C. E.; Wojciechowska, J. K.; Michalak, B.; Kala, E. P.; Kononowicz, K. K. *Eur. J. Med. Chem.* **2003**, *38*, 397.
47. Klotz, K. N. *Naunyn-Schmiedebergs Arch. Pharmacol.* **2000**, *362*, 382.
48. Grover, S.; Bakshi *Pharm. Sci. Technol. Today* **2000**, *3*, 28.
49. González, M. P.; Diaz, H. G.; Molina, R. R.; Cabrera, M. A.; Ramos, A. R. *J. Chem. Inf. Comput. Sci.* **2003**, *43*, 1192.
50. Moro, S.; van Rhee, A. M.; Sanders, L. H.; Jacobson, K. A. *J. Med. Chem.* **1998**, *41*, 46.
51. Roy, K. *Indian J. Chem.* **2003**, *42B*, 1485.
52. Bhattacharya, P.; Roy, K. *Bioorg. Med. Chem. Lett.* **2005**, *15*, 3737.
53. Roy, K. *QSAR Comb. Sci.* **2003**, *22*, 614.
54. Roy, K.; Leonard, J. T.; Sengupta, C. *Bioorg. Med. Chem. Lett.* **2004**, *14*, 3705.
55. Li, A. H.; Moro, S.; Forsyth, N.; Melman, N.; Ji, X. D.; Jacobson, K. A. *J. Med. Chem.* **1999**, *42*, 706.
56. Bhattacharya, P.; Leonard, J. T.; Roy, K. *Bioorg. Med. Chem.* **2005**, *13*, 1159.
57. Borghini, A.; Pietra, D.; Domenichelli, P.; Bianucci, A. M. *Bioorg. Med. Chem.* **2005**, *13*, 5330.
58. Cerius2 Version 4.10 is a product of Accelrys Inc., San Diego, CA.
59. Roy, P. P.; Leonard, J. T.; Roy, K. *Chemom. Intell. Lab. Syst.* **2008**, *90*, 31.
60. Roy, K. *Expert Opin. Drug Discov.* **2007**, *2*, 1567.
61. Everitt, B.; Landau, S.; Leese, M. *Cluster Analysis*; Arnold: London, 2001.
62. Kubinyi, H.; Hamprecht, F.; Mietzner, A. T. *J. Med. Chem.* **1998**, *41*, 2553.
63. Marshall, G. R. In *3D QSAR in Drug Design—Theory, Methods and Applications*; Kubinyi, H., Ed.; ESCOM: Leiden, 1994; p 117.
64. Roy, P. P.; Roy, K. *QSAR Comb. Sci.* **2008**, *27*, 302.
65. Roy, P. P.; Paul, S.; Mitra, I.; Roy, K. *Molecules* **2009**, *14*, 1660.
66. Mitra, I.; Saha, A.; Roy, K. *Mol. Simul* **2010**, *36*, 1067.
67. Hopfinger, A. J.; Tokarsi, J. S. In *Practical Applications of Computer-aided Drug Design*; Charifson, P. S., Ed.; Marcel Dekker: New York, 1997; p 105.
68. Rogers, D.; Hopfinger, A. J. *J. Chem. Inf. Comput. Sci.* **1994**, *34*, 854.
69. Ghose, A. K.; Crippen, G. M. *J. Comput. Chem.* **1986**, *7*, 565.
70. Hirashima, A.; Eiraku, T.; Kuwano, E.; Eto, M. *Internet Electron. J. Mol. Des.* **2003**, *2*, 511.
71. Wold, S. In *Chemometric Methods in Molecular Design*; van de Waterbeemd, H. E., Ed.; VCH: Weinheim, Germany, 1995; p 195.
72. Fan, Y.; Shi, L. M.; Kohn, K. W.; Pommier, Y.; Weinstein, J. N. *J. Med. Chem.* **2001**, *44*, 3254.
73. MINITAB is statistical software of Minitab Inc., USA.
74. Lenzi, O.; Vittoria Colotta, V.; Catarzi, D.; Varano, F.; Poli, D.; Filacchioni, G.; Varani, K.; Vincenzi, F.; Borea, P. A.; Paoletta, S.; Morizzo, E.; Moro, S. *J. Med. Chem.* **2009**, *52*, 7640.
75. Lednicer, D. In *The Organic Chemistry of Drug Synthesis*; Wiley Interscience: New York, 1999; Vol. 6,